

Bearing capacity of foundation on slope determined by energy dissipation method and model experiments

YANG Xiao-li(杨小礼), WANG Zhi-bin(王志斌), ZOU Jin-feng(邹金锋), LI Liang(李亮)
(School of Civil and Architectural Engineering, Central South University, Changsha 410075, China)

Abstract: To determine the ultimate bearing capacity of foundations on sloping ground surface in practice, energy dissipation method was used to formulate the bearing capacity as programming problem, and full-scale model experiments were investigated to analyze the performance of the soil slopes loaded by a strip footing in laboratory. The soil failure is governed by a linear Mohr-Coulomb yield criterion, and soil deformation follows an associated flow rule. Based on the energy dissipation method of plastic mechanics, a multi-wedge translational failure mechanism was employed to obtain the three bearing capacity factors related to cohesion, equivalent surcharge load and the unit gravity for various slope inclination angles. Numerical results were compared with those of the published solutions using finite element method and those of model experiments. The bearing capacity factors were presented in the form of design charts for practical use in engineering. The results show that limit analysis solutions approximate to those of model tests, and that the energy dissipation method is effective to estimate bearing capacity of soil slope.

Key words: energy dissipation; bearing capacity; soil slope; model experiment

1 Introduction

In foundation design, the ultimate bearing capacity of a strip footing is expressed as the sum of the three contributions related to cohesion, surcharge and unit gravity according to TERZAGHI's classical equation. Using TERZAGHI's equation, the bearing capacity is underestimated. Many investigations were performed to modify and extend the TERZAGHI's solution using limit equilibrium method^[1–3], characteristic method^[4–5], limit analysis method^[6–8] and numerical methods based on either the finite element or finite difference^[9]. These investigations are only valid for a situation where the foundations are placed on horizontal ground surfaces.

In practice, the determination of the bearing capacity factors for foundations on soil slope is a very important issue for most engineers. For example, many bridge abutments, building and retaining walls involve the construction of strip footing on soil slopes. However, the research was limited in this area. MICHALOWSKI^[8] presented the numerical results and a closed-form solution for a strip footing on horizontal ground surface using the kinematical approach. ZHU^[3] also presented the numerical results using limit equilibrium method. YANG et al^[10–17] analyzed the slope stability using the energy dissipation method.

In this study, the bearing capacity factors of a strip

footing on soil slope were investigated in the framework of limit analysis theory and full-scale model experiments. The strip shallow footing was placed on homogenous and isotropic soil slope.

2 Energy dissipation analysis

The energy dissipation theorem states that the rate of work done by actual forces is less than or equal to that of energy dissipation in any kinematically admissible velocity fields. A kinematically admissible velocity field is governed by the normality rule and is compatible with the velocities at the boundary of the soil mass. The application of the energy dissipation theorem leads to upper bounds to the true limit load acting on the materials which are assumed to obey Mohr-Coulomb failure criterion in conjunction with the associated flow rule. The lowest possible energy dissipation solution is sought with an optimization scheme by trying various possible kinematically admissible failure mechanisms.

The ultimate bearing capacity q_u of the footing is equal to the vertical ultimate load that the foundation can withstand at the state of incipient failure divided by the base area of the strip footing, which can be written as

$$q_u = cN_c + q_0N_q + 0.5\gamma B_0N_\gamma \quad (1)$$

where B_0 is the footing width; N_c , N_q and N_γ are the bearing capacity factors related to the cohesion c , the

equivalent surcharge load q_0 and the unit gravity γ , respectively.

A multi-wedge translation failure mechanism is often used to calculate bearing capacity of a strip foundation resting on horizontal ground surface. In the present analysis, the multi-wedge failure mechanism is extended to analyze bearing capacity factors of a strip footing on soil slope, as shown in Fig.1, where θ is slope angle, and φ is friction angle. The potential sliding soil is divided into a number of triangular wedges by a series of inclined straight lines. Each of triangular wedges moves as a rigid wedge. The geometry of the i th wedge is characterized by the length of base d_i , angles α_i and β_i , and the length of interface L_i ($i=1, \dots, n$). The angles α_i and β_i ($i=1, \dots, n$) are unspecified. The wedge velocity and relative velocity of the i th wedge with respect to the $(i+1)$ th wedge along the interface are given by the following expressions^[3, 8]:

$$v_{i+1} = \frac{\sin(\alpha_i + \beta_i - 2\varphi)}{\sin(\beta_{i+1} - 2\varphi)} v_i \quad (2)$$

$$v_{i,i+1} = \frac{\sin(\alpha_i + \beta_i - \beta_{i+1})}{\sin(\beta_{i+1} - 2\varphi)} v_i \quad (3)$$

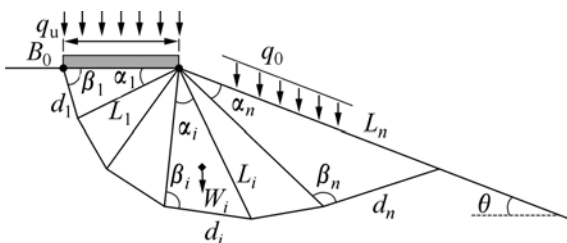


Fig.1 External forces for failure mechanism of footing on soil slope

According to Eqns.(2) and (3), if the velocity v_1 of the first wedge is given, the velocities and relative velocities of all wedges can be gotten by using Eqns.(2) and (3) repeatedly. In general, the velocity v_1 of the first wedge is assumed to be unit for convenience.

The work rate done by the external load and internal energy dissipation rates can be calculated by superposition. The external rate of work is done by the surcharge q_0 on the inclined surface, the soil mass gravity W_i ($i=1, \dots, n$), and the ultimate bearing capacity q_u . Since the soil mass is regarded as perfectly rigid and no general plastic deformation is permitted to occur, the internal energy is dissipated only along velocity discontinuity d_i ($i=1, \dots, n-1$) between the soil at rest and the soil in motion, and along the relative velocity discontinuity interface L_i ($i=1, \dots, n$) between adjoining two wedges.

Equating the work rate of external loads to the total internal energy dissipation rates, the upper bound to the limit load can be obtained. The lowest energy dissipation solution can be obtained by minimizing the limit load.

3 Model experiments

The geometry of the soil slope and the loading equipment are as follows: The model's instrument size (length \times width \times height) is 160 cm \times 160 cm \times 200 cm. The model's gradient and the form of slope foundation are the same as that of original, which is shown in Fig.1. The height of foundation, and the height and the width of soil slope of model are proportional to original sizes by 1:20, respectively. Fig.2 shows the general arrangement including the slope angle and load configuration for the present model experiments. The slopes were constructed with coarse sand backfill. The strip footing on the soil slope was loaded until the failure point was reached. Full-scale experiments were carried to determine the ultimate bearing capacity of the inclination foundation. The geometry of the model test is illustrated in Fig.2, and the instrument arrangement for slope is shown in Fig.3.

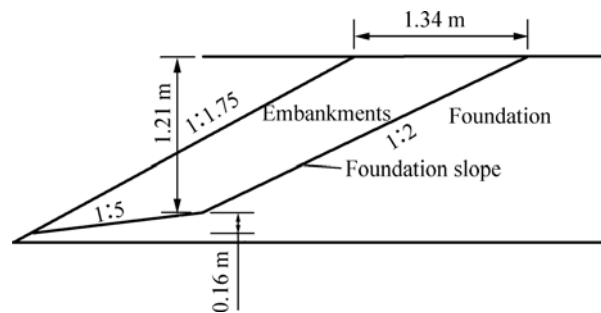


Fig.2 Profile of model experiment

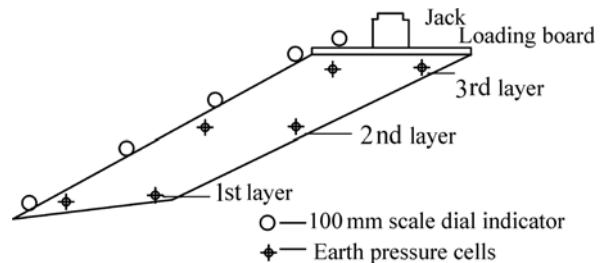


Fig.3 Instrument location of model experiment

A canal with 2 m in depth and 7.5 m in width was excavated along the toe of the embankments in order to reduce the amount of fill required for the embankments to reach failure and to ensure that the failures occurred in the intended direction.

A model canal with 3.0 m in depth and 6 m in

length and 1.6 m in width was constructed in laboratory, three concrete base slabs form a rigid restriction for the soil models. On one side of canal, there are holes for investigating in the slab and organic glasses bestrewed in them.

Slope frame was made up of sand soil and concrete. The proportion between concrete and sand soil was 5:100. Then steps were made on the slope with both length and height of 20 cm. At last 40 cm thick trial soil of detritus air-slaked by red sandstone was covered on the slope and compacted. The soil slope for the test is shown in Fig.2. Experiment material is red soil sandstone. The properties of physical and mechanical of material are listed in Table 1.

Table 1 Properties of soil material

Gravity /($\text{kN}\cdot\text{m}^{-3}$)	Optimum moisture content/%	Liquid limit/%	Plastic limit/%
24.0	8.0	27.9	17.9
Friction angle/($^{\circ}$)	Cohesion/kPa	Plasticity index	
8.0	29.0	10.0	

4 Numerical results

By the energy dissipation theorem of limit analysis, numerical results can be obtained by optimization. For the multi-wedge translational failure mechanism shown in Fig.1, the energy dissipation solutions can be obtained by minimizing objective function with respects to α_i and β_i ($i=1, \dots, n$). The energy dissipation solution can be improved by increasing the number of triangular wedges n . In the present calculations, the triangular wedge number n is equal to 15, which means that the minimization procedure is made with regard to 30 variables and a constraint ($\sum \alpha_i = \pi - \theta$, see Fig.1). From the following comparisons, it can be seen that the number of triangular wedges $n=15$ is sufficient.

Numerical results are summarized in Table 2. Example problems were selected to include the following aspects: 1) comparisons were made between the present solutions and the published solutions, and 2) numerical results for various inclination angles were presented for practical use.

For foundation on soil slope, the present solution using the kinematical approach were presented and compared with the published solutions^[3-8]. Comparisons of static bearing capacity factors N_r are listed in Table 2. It is found that the present solutions agree well with those of MICHALOWSKI^[8] and ZHU^[3].

Using the full-scale model experiments, it is also found that the numerical results almost agree well with

the test results, with the difference being less than 12%.

Fig.4 shows the critical slip surfaces corresponding to $\theta=20^{\circ}$ and $\varphi=35^{\circ}$. From Fig.4, it is found that failure surfaces using the energy dissipation method approximate to that using the model test. In the Fig.4, Fig.4(a) does not consider the effects of the surcharge load and soil gravity, which indicates $q_0=\gamma=0$, however, Fig.4(b) considers the effects. The difference may be caused by the surcharge load and soil gravity of the slope.

Table 2 Comparisons of N_r for foundation on horizontal ground surface

$\varphi/(^{\circ})$	ZHU ^[3]		Present solution	MICHALOWSKI ^[8]	
	Symmetrical	One-side		Numerical	Closed-form
10	0.706	0.845	0.846	0.706	0.840
20	4.466	4.659	4.668	4.468	4.523
30	21.384	21.805	21.874	21.394	21.348
40	111.750	120.150	120.863	118.827	118.199
50	1 025.064	1 033.480	1 046.000	1 025.980	1 017.676

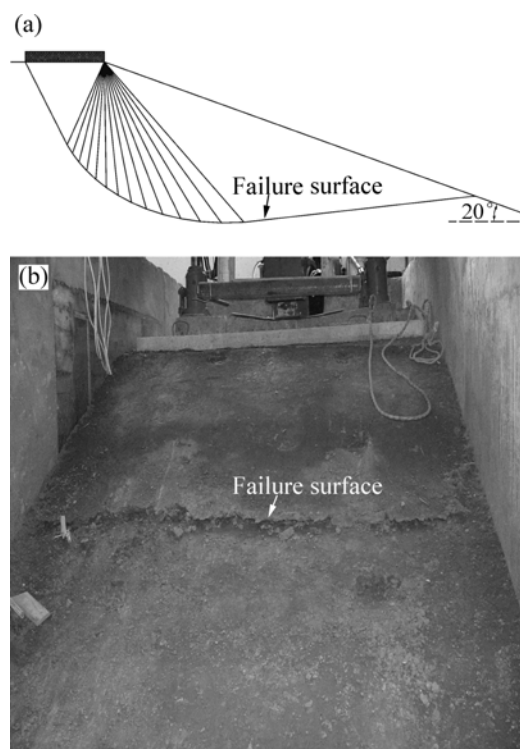


Fig.4 Comparison of two failure surfaces
 (a) Slip surface using energy dissipation method;
 (b) Slip surface using model test

Using the energy dissipation method, some numerical results were used to calculate the three bearing capacity factors of a strip footing on soil slope, and some charts relating bearing capacity factors N_c , N_q and N_r to various parameters φ and θ are presented in Fig.5. These charts are given for practical use in geotechnical engineering.

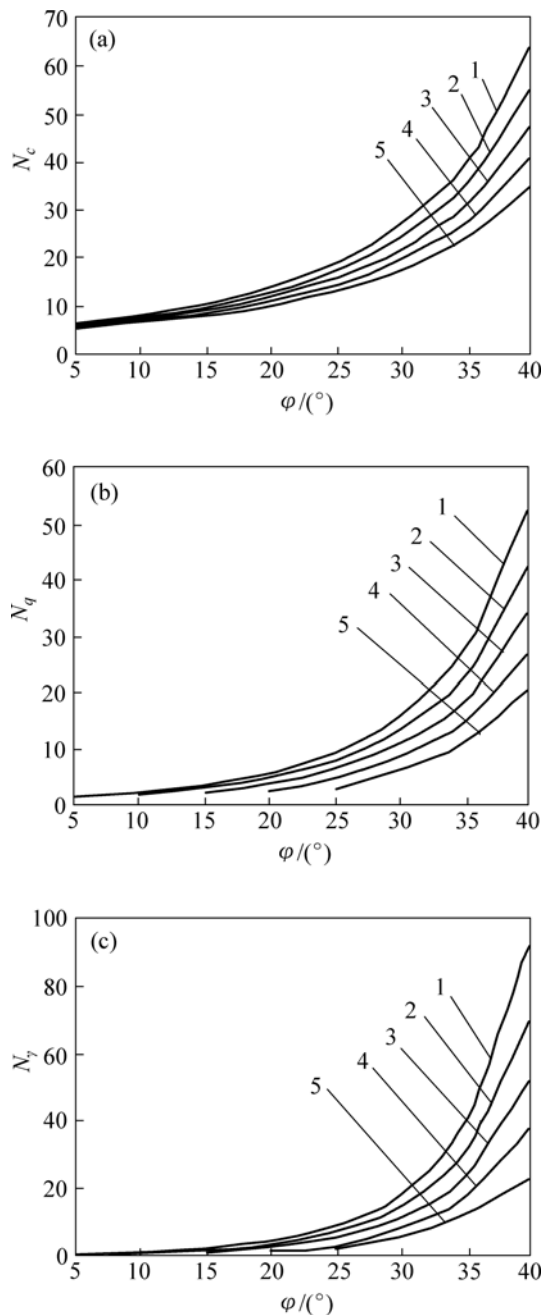


Fig.5 Design charts for three bearing capacity factors N_c , N_q and N_y of strip footing on soil slope with different slope angles(θ)
 θ ($^\circ$): 1—5; 2—10; 3—15; 4—20; 5—25

5 Conclusions

1) Incorporating the effect of various slope inclination angles, the bearing capacity factors of a strip footing are investigated using an energy dissipation method of plasticity and full-scale model experiments.

2) Energy dissipation solutions are obtained by optimization, and are compared with the model experiment results. The failure mechanism using the energy dissipation theorem is also compared with the

mechanism observed by measurements. The good agreement shows that the energy dissipation method is an effective method to estimate bearing capacity factors of a strip footing on soil slope.

3) The work on calculation of the bearing capacity factors of the foundation on horizontal ground surface is extended to that on soil slopes, and ends with the presentation of design charts for the bearing capacity factors for practical use in engineering.

References

- [1] YANG Xiao-li. Upper bound analysis of active earth pressure with different fracture surface and nonlinear yield criterion[J]. *Theoretical and Applied Fracture Mechanics*, 2007, 47(1): 46–56.
- [2] BUDHU M, AL-KARNI A. Seismic bearing capacity of soils[J]. *Geotechnique*, 1993, 43(2): 181–187.
- [3] ZHU D Y. The least upper bound solutions for bearing capacity factor N_r [J]. *Soils and Foundations*, 2000, 40(1): 123–129.
- [4] MICHALOWSKI R L, PARK N. Admissible stress fields and arching in piles of sand[J]. *Geotechnique*, 2004, 54(8): 529–538.
- [5] BOLTON M D, LAU C K. Vertical bearing capacity factors for circular and strip footings on Mohr-Coulomb soil[J]. *Canadian Geotechnical Journal*, 1993, 38(5): 1090–1096.
- [6] CHEN W F. *Limit analysis and soil plasticity*[M]. Amsterdam: Elsevier Scientific Publishing Company, 1975: 1–80.
- [7] UKRITCHON B, WHITTLE A J, KLANGVIJIT C. Calculations of bearing capacity factor using numerical limit analysis[J]. *Journal of Geotechnical and Geoenvironmental Engineering*, 2003, 129(5): 468–474.
- [8] MICHALOWSKI R L. An estimate of the influence of soil weight on bearing capacity using limit analysis[J]. *Soils and Foundations*, 1997, 37(4): 57–64.
- [9] YIN Jian-hua, WANG Yue-jie, SELVADURAI A P. Influence of non-association on bearing capacity of a strip footing[J]. *Journal of Geotechnical and Geoenvironmental Engineering*, 2001, 127(11): 985–989.
- [10] YANG Xiao-li, ZOU Jin-feng. Stability factors for rock slopes subjected to pore water pressure based on the Hoek-Brown failure criterion[J]. *International Journal of Rock Mechanics and Mining Sciences*, 2006, 43(7): 1146–1152.
- [11] YANG Xiao-li, YIN Jian-hua. Estimation of seismic passive earth pressure with non-linear failure criterion[J]. *Engineering Structures*, 2006, 28(3): 342–348.
- [12] YANG Xiao-li, YIN Jian-hua. Linear Mohr-Coulomb strength parameters from the nonlinear Hoek-Brown rock masses[J]. *International Journal of Non-linear Mechanics*, 2006, 41(8): 1000–1005.
- [13] YANG Xiao-li, YIN Jian-hua. Upper bound solution for ultimate bearing capacity with a modified Hoek-Brown failure criterion[J]. *International Journal of Rock Mechanics and Mining Sciences*, 2005, 42(4): 550–560.
- [14] YANG Xiao-li, LI Liang, YIN Jian-hua. Stability analysis of rock slopes with a modified Hoek-Brown failure criterion[J]. *International Journal for Numerical and Analytical Methods in Geomechanics*, 2004, 28(2): 181–190.
- [15] YANG Xiao-li, LI Liang, YIN Jian-hua. Seismic and static stability analysis for rock slopes by a kinematical approach[J]. *Geotechnique*, 2004, 54(8): 543–549.
- [16] YANG Xiao-li, YIN Jian-hua. Slope stability analysis with nonlinear failure criterion[J]. *Journal of Engineering Mechanics*, 2004, 130(3): 267–273.
- [17] YANG Xiao-li, YIN Jian-hua, LI Liang. Influence of a nonlinear failure criterion on the bearing capacity of a strip footing resting on rock mass using a lower bound approach[J]. *Canadian Geotechnical Journal*, 2003, 40(3): 702–707.

(Edited by CHEN Can-hua)